Check for updates

Flexural Behavior of Reinforced Concrete Beams Strengthened by Textile Reinforced Magnesium Potassium Phosphate Cement Mortar

Cheng-Jie Zhu[1,2], Shuai Fang[3]*, P. L. Ng[2,4]*, Ina Pundienė[2] and Jia-Jian Chen[5]

[1] College of Civil Engineering, Yancheng Institute of Technology, Yancheng, China, [2] Institute of Building Materials, Vilnius Gediminas Technical University, Vilnius, Lithuania, [3] School of Civil Engineering and Transportation, South China University of Technology, Guangzhou, China, [4] Department of Civil Engineering, The University of Hong Kong, Hong Kong, China, [5] Department of Civil Engineering, Foshan University, Foshan, China

Magnesium potassium phosphate cement (MKPC), made of sintered magnesium oxide and potassium phosphate, is a new material for construction and structural repair. It possesses high early strength and bond capacity, low drying shrinkage, excellent fire resistance and compatibility with concrete. These characteristics render it an ideal material for strengthening reinforced concrete (RC) structures. This study developed a MKPC-based textile reinforced cementitious composite (TRCC) to strengthen RC beams at soffit. Three-point flexural tests were conducted on two control specimens without strengthening and two strengthened specimens. Experimental results showed that the TRCC system exhibits good bonding with substrate concrete. The strengthened specimens failed due to rupture of textile meshes in TRCC. TRCC could improve load capacity by 4–25%, postpone propagation of cracks, reduce tensile strain of main reinforcement and reduce deflection of beams at the same load level. High relative textile ratios contributed to the load resistance while impaired the ductility of strengthened beams. Design formulae are proposed to predict the flexural capacity of beams strengthened by MKPC-based TRCC, and reasonable prediction close to experimental results can be obtained from the formulae.

Keywords: flexural ductility, flexural strengthening, magnesium potassium phosphate cement, relative textile ratio, textile reinforced cementitious composite

INTRODUCTION

Reinforced concrete (RC) structures are susceptible to structural deterioration due to aging, earthquake, fire, and chemical corrosion. Researchers and engineers have been seeking effective and economical methods for strengthening deteriorated structures. A new textile reinforced cementitious composite (TRCC) strengthening system has drawn attention recently (Bernat et al., 2013; Escrig et al., 2015; Mesticou et al., 2017; Ortlepp and Ortlepp, 2017; Holschemacher et al., 2018). It consists of cementitious matrix reinforced with textile meshes, and it possesses good performance under both compression and tension (Triantafillou, 2016). TRCC has advantages of

desirable durability, ease of construction and high strengthening efficiency (Yin, 2010; Cao, 2015; Holschemacher, 2020). The cementitious binder of TRCC has excellent durability, fire resistance and compatibility with concrete structures (Xu et al., 2016; Kong et al., 2017; Tran et al., 2018). The common fibers used in TRCC, such as carbon fiber, alkali-resistant (AR) glass fiber, aramid fiber and basalt fiber, possess outstanding corrosion resistance (Mobasher, 2019; Peled et al., 2019). This enables adoption of thin cover for TRCC, which can least affect the original dimensions of members due to strengthening (Hegger and Voss, 2008; Yin et al., 2019). In addition, the orientations and layers of textile meshes can be easily adjusted according to the stress distribution of strengthened members (Bruckner et al., 2006). The above-mentioned advantages facilitate the application of TRCC in structural repair and strengthening (Naaman, 2010).

Different researchers have conducted studies on the mechanical performance of TRCC strengthened RC members. They found that TRCC can effectively enhance the cracking load, yield load and ultimate load of RC beams (Zhang, 2009; Xun et al., 2010; Zhi et al., 2017). In comparison with FRP (fiber-reinforced polymer) system, TRCC strengthening was reported to exhibit a slightly inferior improvement in load capacity, but better crack resistance and more ductile failure mode than FRP (Yin et al., 2015; Raoof et al., 2017). Kolsch (1998) indicated that the bond between TRCC and substrate concrete acts as a critical factor for effective repair and strengthening. According to Zhang (2009) and Xun et al. (2010), upon increasing the textile mesh ratios to a certain level, the bond becomes a limiting factor controlling the load capacity of strengthened members.

Magnesium potassium phosphate cement (MKPC) is made of sintered magnesium oxide and potassium phosphate (Gardner et al., 2015; Le Rouzic et al., 2017; Yang et al., 2020). As compared with ordinary Portland cement, MKPC has higher bond strength, lower drying shrinkage, faster setting and better abrasive resistance, which makes MKPC a highly competitive binder for TRCC system (Cao, 2015; Du et al., 2017). This study put forward a new strengthening scheme using MKPC-based TRCC and investigated its strengthening effect on RC beams. Control and strengthened RC beams were produced and subjected to flexural tests. The experimental results exhibited good agreement with the design formulae for flexural strengthening proposed in this research.

EXPERIMENTAL INVESTIGATION

Materials and Specimens

The component materials for preparation of TRCC included MKPC paste (used as bond coat applied onto the substrate concrete) and MKPC mortar (applied upon placing each layer of textile mesh), and fabric textile meshes. The ingredients and mix proportions of MKPC paste and mortar can be referred to the research works by Gu (2019), and are complying with the requirements in Chinese Standard JC/T 2537-2019 (Ministry of Industry and Information Technology of the People's Republic of China [MOIIT], 2019). The mix proportions of the MKPC paste and mortar, and their mean flexural strengths and mean

compressive strengths at 28 days are given in **Table 1**. The flexural strengths of MKPC paste and mortar were measured from 40 mm × 40 mm × 160 mm prism specimens under a loading rate of 50 ± 10 N/s according to International Standard ISO 679 (International Organization for Standardization, 2009). Following the same standard, the compressive strengths were measured from the broken prism specimens under a loading rate of 2400 ± 200 N/s. It is noted that the MKPC paste and mortar had higher compressive strength compared to the concrete of the specimen beams, but not excessively high to render the MKPC materials suitable for use in strengthening without compatibility problem.

The fabric textile meshes were woven orthogonally with carbon and AR glass fabric bundles. The former possessed excellent mechanical performance and contributed mainly to load capacity enhancement of strengthened structural members, while the latter was of lower cost and could sustain larger elongation. **Table 2** summarizes the characteristics of textile meshes, of which the tensile properties were measured in laboratory according to the requirements in Chinese Standard GB/T 3362-2017 (General Administration of Quality Supervision, Inspection and Quarantine of the People's Republic of China [GAQSIQ], 2017). The meshes were cut into pieces with dimensions of 1500 × 150 mm, in which carbon fabric bundles were aligned along the longitudinal direction of the beam member. Intervals between fabric bundles were 15 mm in both directions. In order to keep the textile meshes parallel to soffit surface and even out the load distribution among the fabric bundles, the meshes were stiffened by impregnation in epoxy resin. The fabric bundles were maintained straight during the curing and hardening of epoxy resin.

The beam specimens were 2000 mm long and had a uniform cross section of 150 mm (breadth) × 250 mm (depth). Reinforcements of specimen consisted of two main reinforcing bars at tension side, two hanger bars and 16 stirrups. The stirrups had center-to-center spacing of 200 mm at the mid-span region and 100 mm approaching both ends of specimens (**Figure 1**). Deformed steel bars with diameters of 10 and 16 mm (D10 and

TABLE 1 | Mix proportions and strength of MKPC paste and mortar.

	MKPC paste	MKPC mortar
Magnesium oxide	0.8	0.8
Fly ash	0.1	0.1
Metakaolin	0.1	0.1
Potassium dihydrogen phosphate	0.4	0.667
Borax	0.025	0.02
Disodium hydrogen phosphate	0.07	0.08
Inorganic chloride-containing salt	0.03	0.04
Sodium silicate solution	0.031	0.036
Water	0.229	0.325
Sand	–	1.25
28-day flexural strength (MPa)	8.13	6.97
28-day compressive strength (MPa)	50.15	61.69

In the mix proportions, the values shown are mass ratios with respect to the contents of (Magnesium oxide + Fly ash + Metakaolin).

TABLE 2 | Characteristics of textile mesh.

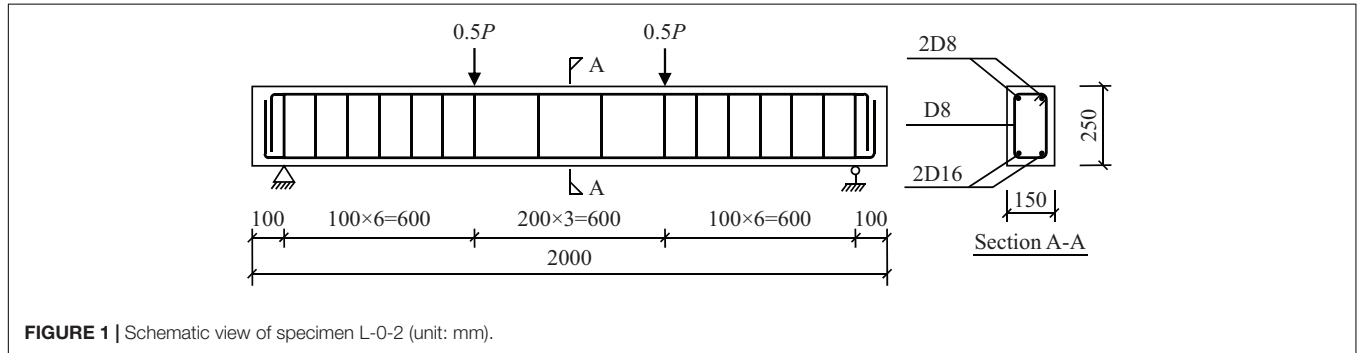| Fiber direction	Fiber type	Sectional area (mm²/bundle)	Tensile strength f_{cf} (MPa)	Elastic modulus (GPa)	Elongation
Longitudinal	Carbon fiber	0.45	2184.4	236	1.2%
Transverse	AR glass fiber	0.58	698.3	65	2.5%

FIGURE 1 | Schematic view of specimen L-0-2 (unit: mm).

TABLE 3 | Details of main reinforcements and textile meshes.

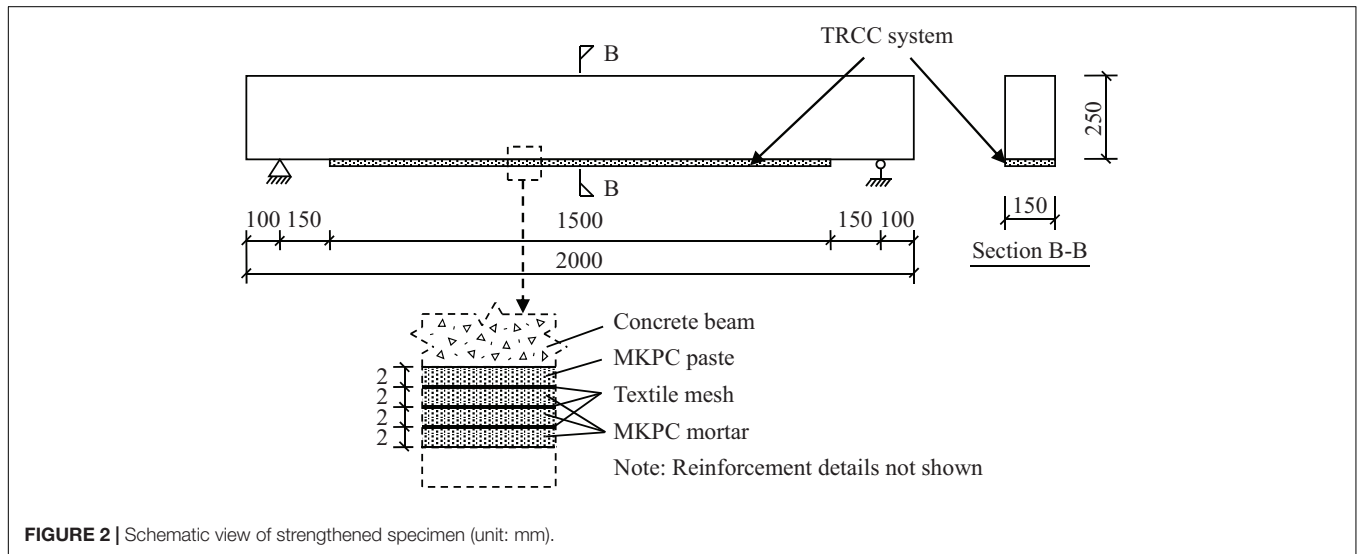| Specimen	Main reinforcement	Main reinforcement ratio	Layer of textile mesh	Textile ratio	Relative textile ratio
L-0-1	2D10	0.494%	-	-	-
LD-3	2D10	0.494%	3	0.047%	9.51%
L-0-2	2D16	1.283%	-	-	-
LD-2	2D16	1.283%	2	0.032%	2.49%

FIGURE 2 | Schematic view of strengthened specimen (unit: mm).

D16) were used as the main reinforcements of RC beams. Plain steel bars with diameter of 8 mm (D8) were used as hanger bars and stirrups. The average yield strength of D8, D10, and D16 bars were measured from tensile testing in laboratory to be 479.34, 511.20, and 534.25 MPa, respectively. Concrete cover for stirrups was 25 mm. The 28-day mean compressive strength of concrete measured from 150 mm cubes was 44.77 MPa.

Four RC beam specimens were prepared. Two beams (L-0-1 and L-0-2) with different main reinforcement ratios were designated as control specimens. The remaining two specimens (LD-3 and LD-2) were strengthened using TRCC with three and two layers of meshes, respectively. **Table 3** summarizes the main reinforcement and textile mesh details of the specimens. Specimens L-0-1 and LD-3 had the same main reinforcement ratio, whereas specimens L-0-2 and LD-2 had the same main reinforcement ratio. Main reinforcement ratios and textile ratios are defined as the ratios of sectional area of main reinforcements and longitudinal fabric bundles to the effective area of beam section, respectively. Relative textile ratio denotes the sectional area ratio of longitudinal fabric bundles to main reinforcements.

Strengthening

Strengthening with TRCC was applied to specimens LD-3 and LD-2. The strengthening work consisted of the following steps. Firstly, the specimens were inverted with their soffits facing upwards. The soffit surface was then mechanically chiseled for roughening. The chiseled region had a length of 1500 mm and a width of 150 mm (**Figure 2**). MKPC paste with thickness of 2 mm was applied on the chiseled region as the bond coat for better surface bonding. One layer of impregnated textile mesh was laid on the MKPC paste. Subsequently, MKPC mortar with thickness of 2 mm was applied to cover the mesh. The preceding steps of laying the textile mesh and covering with MKPC mortar were repeated until the required number of textile mesh layers was completed. **Figure 2** illustrates the strengthening scheme. After final setting, the MKPC-based TRCC were kept dampened for 28 days.

Experimental Setup

Strain gauges were installed on main reinforcements. Displacement gauges were installed at mid-span and support positions to record the deflection of beam specimens. Three-point flexural tests were performed on the specimens. **Figure 3** depicts the schematic view of the flexural test. During the test, monotonic load with an increment step of 5 kN was applied to the specimens. The tests were terminated when the specimens failed to carry the imposed load.

RESULTS AND DISCUSSION

Failure Modes

Both control specimens L-0-1 and L-0-2 exhibited typical bending failure. As the load increased, the cracks initiated at the soffit of specimens and propagated upwards. The cracks were distributed in pure bending zone of the specimens. When the load reached the yielding level, main reinforcements yielded and deflection of specimens rapidly increased. Finally the concrete in the compression region of specimens crushed (**Figures 4A,C**).

For the strengthened specimens LD-3 and LD-2, benefited from the structural resistance of TRCC, the flexural strengthening

postponed the cracking of concrete. As compared with the control specimens, the strengthened beams showed more cracks at smaller intervals. Failure of both strengthened specimens was initiated by yielding of main reinforcements, and followed by rupture of textile meshes in TRCC and then crushing of concrete in compression region. The bond between TRCC and strengthened specimens remained intact during the tests and there was no sign of bond failure (**Figures 4B,D**).

Load-Deflection Relationships

The experimentally obtained load-deflection relationships of specimens are plotted in **Figure 5**. In the elastic stage, the control and strengthened specimens had similar deflections. After cracking of concrete, the flexural tensile stress was carried by main reinforcements and textile meshes at cracked sections. Comparative study of the specimens reflected that, the higher the relative textile ratio was, the larger was the difference in deflections between control and strengthened specimens. When the main reinforcements yielded, the deflection increased sharply. A typical yielding plateau was observed from the load-deflection curve of specimen L-0-1. In contrast, strengthened specimens LD-3 and LD-2 exhibited much smaller ultimate deflections due to smaller elongation of longitudinal carbon fabric bundles. Among the pair of strengthened specimens, it held true that higher relative textile ratio resulted in higher strengthening efficiency. Evidently, specimen LD-3 achieved greater improvement in both the load capacity and flexural stiffness than specimen LD-2.

Tensile strain of main reinforcements was measured and plotted in **Figure 6**. Benefited from the contribution by textile meshes in jointly resisting tensile stresses, the main reinforcements in strengthened specimens sustained lower tensile strain than those in control specimens under the same load level. As the relative textile ratio increased, the difference in the reinforcement strains between strengthened and control specimens enlarged. Testing of additional strengthened beam specimens would be desirable in order to quantitatively establish the relative contributions of textile meshes and main reinforcements to the load resistance at various load levels.

Load Capacity and Ductility

Cracking load P_{cr}, yield load P_y, and ultimate load P_u obtained from testing of specimens are summarized in **Table 4**. The cracking load and yield load are the load at which the specimens crack and main reinforcements yield, respectively. The ultimate load is the maximum load carried by the specimens. It can be seen that the load capacity of specimens achieved varying degrees of improvement by TRCC strengthening. TRCC with relative textile ratio of 2.49% could increase the cracking load, yield load and ultimate load by 26.8, 7.7, and 4.3%, respectively. As the relative textile ratio was increased to 9.51%, the above improvement in load resistances increased, respectively, to 86.4, 54.0, and 25.0%. The maximum percentage of improvement was observed in cracking load, followed by yield load, and ultimate load ranked the last. This is because carbon fabric bundles at beam soffit had higher elastic modulus and larger lever arm than main reinforcements. The bundles, therefore, played primary
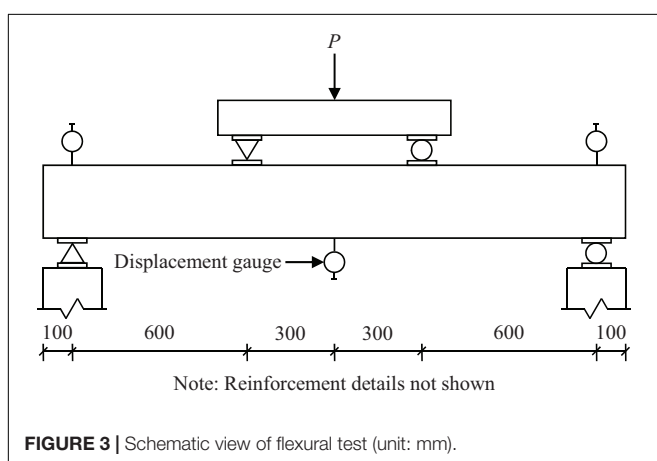

P

Displacement gauge

100 600 300 300 600 100

Note: Reinforcement details not shown

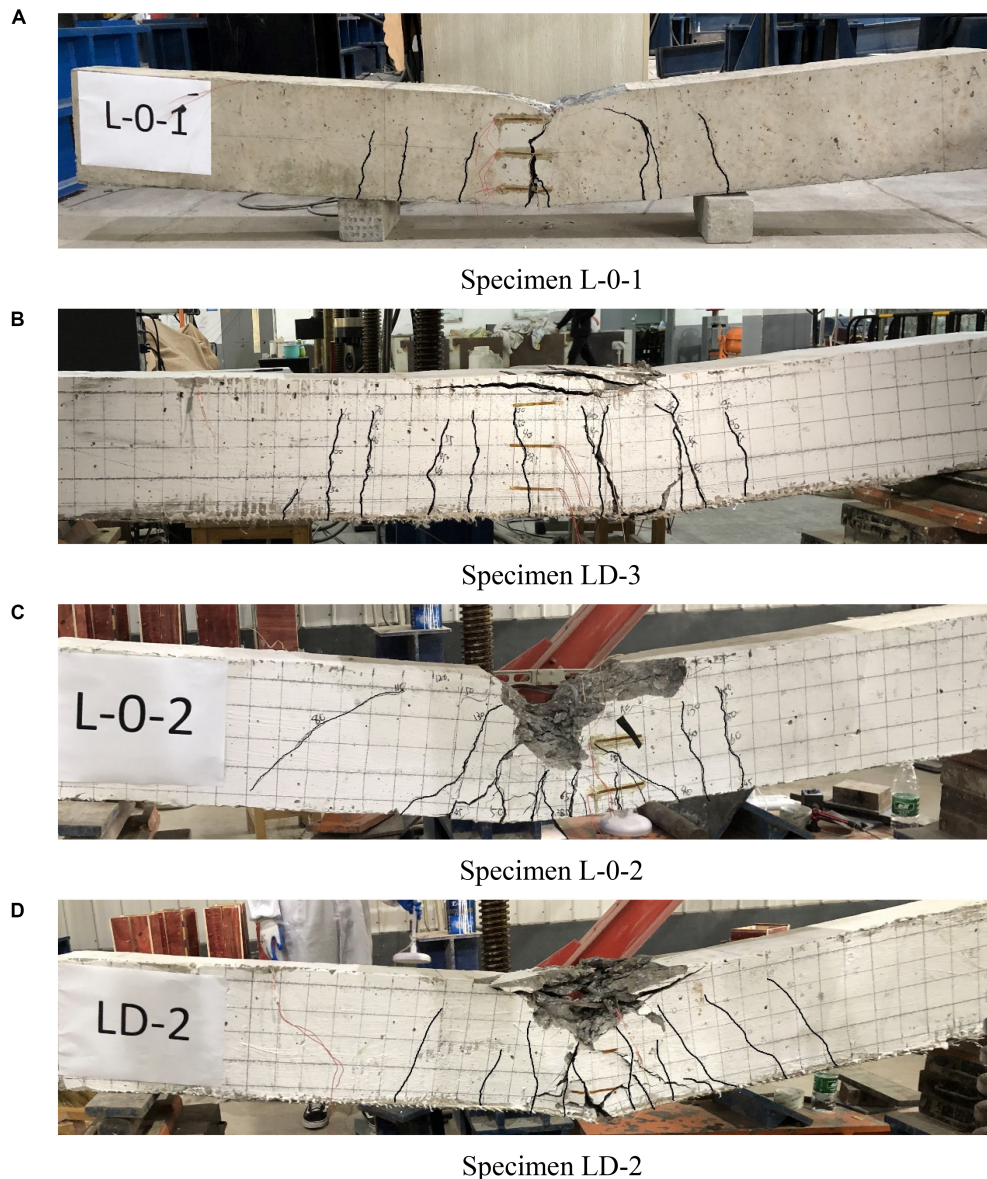**FIGURE 3 |** Schematic view of flexural test (unit: mm).

FIGURE 4 | Failure modes of specimens. **(A)** Specimen L-0-1. **(B)** Specimen LD-3. **(C)** Specimen L-0-2. **(D)** Specimen LD-2.

role in resisting load in the initial stage of flexural test. As the load increased, the neutral axis of beams gradually shifted upwards. Main reinforcements then played more significant role in contributing to the load resistance, and the role of fabric bundles became less significant.

Corresponding to P_{cr}, P_y, and P_u, the values of cracking deflection Δ_{cr}, yield deflection Δ_y, and ultimate deflection Δ_u are summarized in **Table 5**. Experimental results indicated that TRCC strengthening enhanced stiffness and postponed both cracking and yielding of specimens. To evaluate the flexural ductility of specimens, the ductility factor is obtained as Δ_u divided by Δ_y and are reported in the last column of **Table 5**. The results reflected that the ductility factor of strengthened specimen LD-3 decreased by 79% as compared with that

of control specimen L-0-1. Due to the small elongation of longitudinal carbon fabric bundles, the strengthened specimen did not exhibit high ductility.

PREDICTION OF FLEXURAL CAPACITY OF STRENGTHENED BEAMS

Based on the formulation for flexural capacity of RC beams in Chinese Standard GB 50010-2010 (Ministry of Housing and Urban-Rural Development of the People's Republic of China [MOHURD], 2010) provisions, design formulae for flexural capacity of TRCC strengthened beams is proposed. Tensile strength of carbon fabric bundles is taken into consideration in
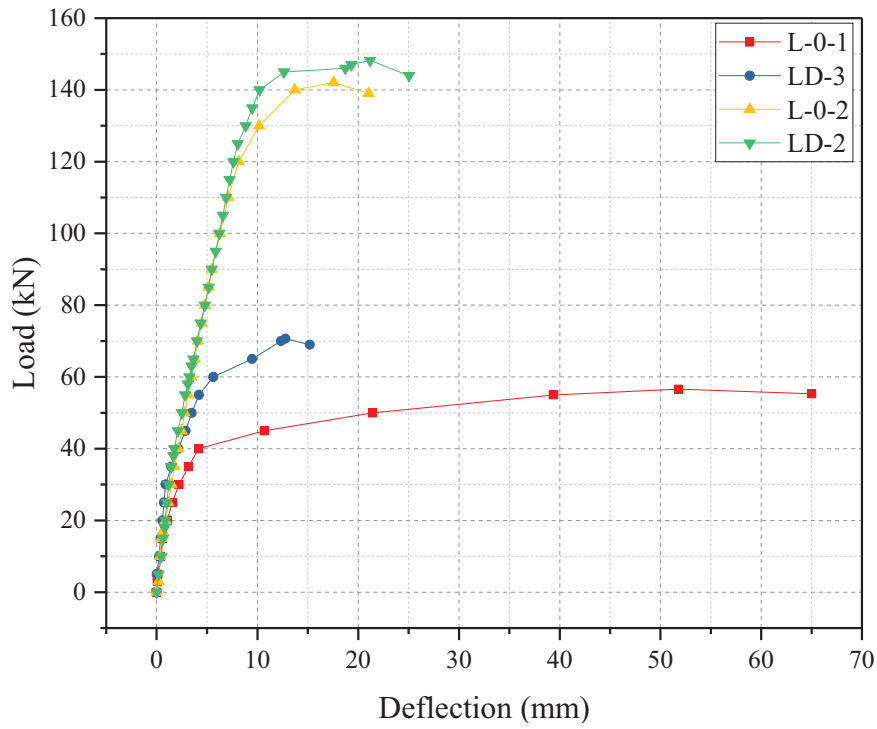
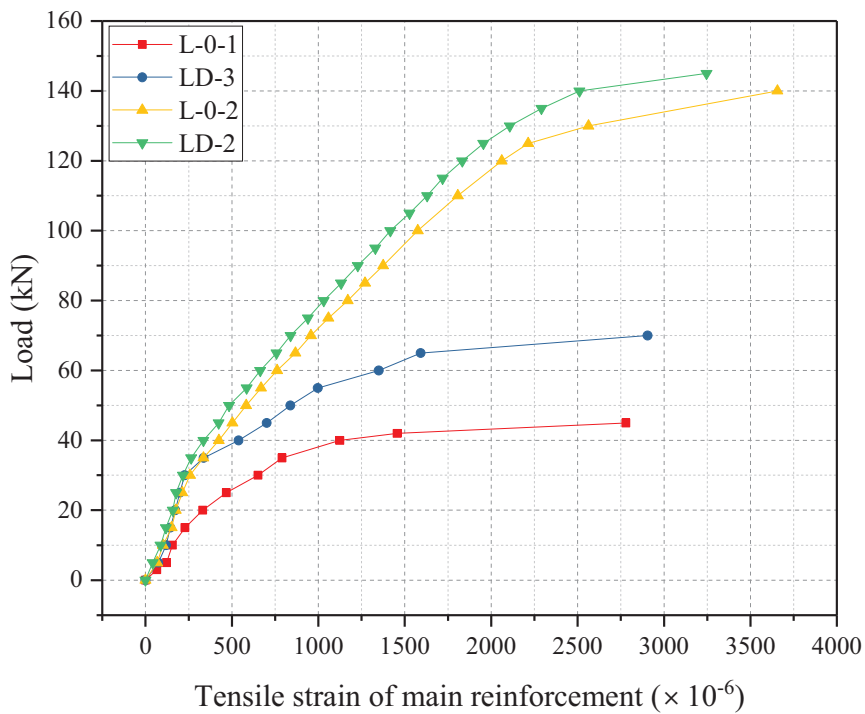**FIGURE 5 |** Relationships between load and deflection.

FIGURE 6 | Relationships between load and tensile strain of main reinforcement.

Specimen	P_{cr} (kN)	Increment	P_y (kN)	Increment	P_u (kN)	Increment
L-0-1	17.51	–	44.28	–	56.57	–
LD-3	32.64	86.4%	68.21	54.0%	70.69	25.0%
L-0-2	28.56	–	130.99	–	142.08	–
LD-2	36.20	26.8%	141.09	7.7%	148.23	4.3%

TABLE 5 | Deflections and ductility factor of specimens.

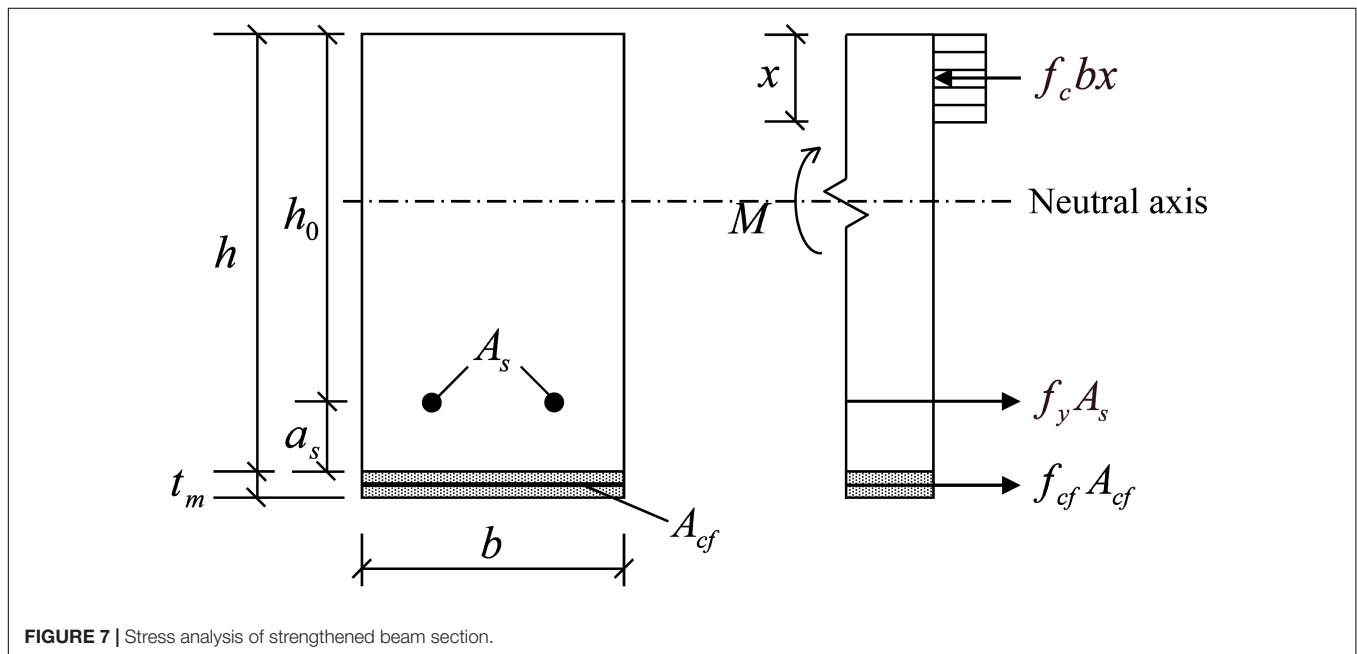| Specimen	Δ_{cr} (mm)	Δ_y (mm)	Δ_u (mm)	Ductility factor
L-0-1	0.82	9.74	51.79	5.32
LD-3	1.18	11.32	12.78	1.13
L-0-2	1.37	10.51	17.55	1.67
LD-2	1.52	10.73	21.17	1.97

FIGURE 7 | Stress analysis of strengthened beam section.

the prediction. According to the failure mode of strengthened beam, stress analysis of the beam sections is conducted, as illustrated in **Figure 7**.

Flexural capacity of strengthened specimens can be predicted by the following equations:

$$f_c bx = f_y A_s + f_{cf} A_{cf} \tag{1}$$

$$M_u = f_c bx \left(h + \frac{t_m}{2} - \frac{x}{2} \right) - f_y A_s \left(h + \frac{t_m}{2} - h_0 \right) \tag{2}$$

where f_c is axial compressive strength of concrete; b and h are width and depth of cross section of beam, respectively, f_y is yield strength of main reinforcements; f_{cf} is tensile strength of carbon fabric bundles; A_s and A_{cf} are sectional area of main reinforcements and carbon fabric bundles, respectively, x is depth of the equivalent rectangular compressive stress block of concrete; t_m is overall thickness of TRCC system; h_0 is the effective depth (i.e., the distance from the extreme compression fiber to the centroid of main reinforcements). The above equations do not account for slippage of reinforcing bar or fabric textile mesh. In carrying out design, attention should be paid to proper reinforcement and fabric mesh detailing against slip failure.

Eqs (1) and (2) can be adopted as design formulae for predicting flexural capacity of MKPC-based TRCC strengthened RC beams. The predicted flexural capacity of specimens LD-2 and LD-3 are 44.15 and 23.84 kNm, with errors of -0.7 and +11.1% as compared with the experimental values of 44.47 and 21.21 kNm, respectively. As reflected from Eqs (1) and (2), the tensile strength of fabric material will affect the flexural capacity of strengthened beams, further research is recommended to investigate the flexural behavior of TRCC strengthened beams using alternative fabric materials.

CONCLUSION

In this paper, a new strengthening system, magnesium potassium phosphate cement or MKPC-based TRCC (textile reinforced cementitious composite) strengthening, was proposed to strengthen RC (reinforced concrete) beams. Two control and two strengthened specimens were produced and subjected to three-point flexural tests. Based on the experimental results, the following conclusions can be drawn:

1. MKPC-based TRCC possessed excellent bonding with substrate concrete. Strengthened beams failed due to rupture of longitudinal carbon fabric bundles in TRCC.
2. MKPC-based TRCC could effectively improve load capacity of RC beams. Relative textile ratio exerted crucial influence on the effectiveness of strengthening. Relative textile ratios at 2.49 and 9.51% resulted in increments of ultimate load of strengthened beams by 4.3 and 25.0%, respectively.
3. The adopted TRCC strengthening system decreased the flexural ductility of RC beams due to the small elongation of longitudinal carbon fabric bundles.

Design formulae were proposed to predict the flexural capacity of beams strengthened by MKPC-based TRCC system. The prediction yielded good agreement with the experimental value of the strengthened specimen, especially for the beam with relative textile ratio of 2.49%. Further research is recommended on the use of alternative fabric materials in the TRCC system for strengthening.

DATA AVAILABILITY STATEMENT

The raw data supporting the conclusions of this article will be made available by the authors, without undue reservation, to any qualified researcher.

AUTHOR CONTRIBUTIONS

C-JZ: conceptualization, data curation, funding acquisition, investigation, methodology, project administration, resources, visualization, and writing – original draft. SF: data interpretation, formal analysis, investigation, methodology, visualization, and writing – original draft. PN: data interpretation, funding acquisition, resources, supervision, validation, and writing – review and editing. IP: conceptualization, formal analysis, project administration, resources, supervision, and validation. J-JC: data curation, data interpretation, resources, software, validation, and visualization. All authors contributed to the article and approved the submitted version.

FUNDING

REFERENCES

Bernat, E., Gil, L., Roca, P., and Escrig, C. (2013). Experimental and analytical study of TRM strengthened brickwork walls under eccentric compressive loading. *Constr. Build. Mater.* 44, 35–47. doi: 10.1016/j.conbuildmat.2013.03.006

Bruckner, A., Ortlepp, R., and Curbach, M. (2006). Textile reinforced concrete for strengthening in bending and shear. *Mater. Struct.* 39, 741–748. doi: 10.1617/s11527-005-9027-2

Cao, D. W. (2015). *Research and Technology on Bending Performance of Textile Reinforced Magnesium Phosphate Cement Matrix Composites Reinforced Defected Beams*. Ph. D. Thesis, Suzhou University of Science and Technology, Suzhou.

Du, Y. B., Cao, D. W., Xun, Y., Yang, J. M., and Gao, P. W. (2017). Experimental study on shearing bonding behavior between magnesium potassium phosphate cement mortar and concrete. *Build. Struct.* 47, 35–38.

Escrig, C., Gil, L., Bernat, E., and Puigvert, F. (2015). Experimental and analytical study of reinforced concrete beams shear strengthened with different types of textile-reinforced mortar. *Constr. Build. Mater.* 83, 248–260. doi: 10.1016/j.conbuildmat.2015.03.013

Gardner, L. J., Bernal, S. A., Walling, S. A., Corkhill, C. L., Provis, J. L., and Hyatt, N. C. (2015). Characterisation of magnesium potassium phosphate cements blended with fly ash and ground granulated blast furnace slag. *Cem. Concr. Res.* 74, 78–87. doi: 10.1016/j.cemconres.2015.01.015

General Administration of Quality Supervision, Inspection and Quarantine of the People's Republic of China [GAQSIQ] (2017). *GB/T 3362-2017: Test Methods for Tensile Properties of Carbon Fiber Multifilament*. Beijing: Standards Press of China.

Gu, H. J. (2019). *Slurry Design and Properties Experimental Study of High Fluidity Potassium Magnesium Phosphate Cement*. Ph. D. Thesis, Jiangsu University of Science and Technology, Zhenjiang.

Hegger, J., and Voss, S. (2008). Investigations on the bearing behaviour and application potential of textile reinforced concrete. *Eng. Struct.* 30, 2050–2056. doi: 10.1016/j.engstruct.2008.01.006

Holschemacher, K. (2020). Application of textile reinforced concrete in precast concrete industry. *IOP Conf. Ser. Mater. Sci. Eng.* 753:042086. doi: 10.1088/1757-899x/753/4/042086

Holschemacher, K., Meβerer, D., and Heiden, B. (2018). "Test method for curvature-dependent tensile strength reduction of textile reinforced concrete (TRC)," in *Proceeding of the 5th fib Congress, Melbourne, Australia*, (Melbourne, VI: FIB).

International Organization for Standardization (2009). *ISO 679-2009: Cement – Test Methods - Determination of Strength*. Geneva: International Organization for Standardization.

Kolsch, H. (1998). Carbon fiber cement matrix (CFCM) overlay system form masonry strengthening. *J. Compos. Constr.* 2, 105–109. doi: 10.1061/(asce)1090-0268(1998)2:2(105)

Kong, K., Mesticou, Z., Michel, M., Larbi, A., and Junes, A. (2017). Comparative characterization of the durability behaviour of textile reinforced concrete (TRC) under tension and bending. *Compos. Struct.* 179, 107–123. doi: 10.1016/j.compstruct.2017.07.030

Le Rouzic, M., Chaussadent, T., Stefan, L., and Saillio, M. (2017). On the influence of Mg/P ratio on the properties and durability of magnesium potassium phosphate cement pastes. *Cem. Concr. Res.* 96, 27–41. doi: 10.1016/j.cemconres.2017.02.033

Mesticou, Z., Bui, L., Junes, A., and Larbi, A. (2017). Experimental investigation of tensile fatigue behaviour of textile-reinforced concrete (TRC): effect of fatigue load and strain rate. *Compos. Struct.* 160, 1136–1146. doi: 10.1016/j.compstruct.2016.11.009

Ministry of Housing and Urban-Rural Development of the People's Republic of China [MOHURD] (2010). *GB 50010-2010: Code for Design of Concrete Structures*. Beijing: China Architecture & Building Press.

Ministry of Industry and Information Technology of the People's Republic of China [MOIIT] (2019). *JC/T 2537-2019: Magnesium Phosphate Repairing Mortar.* Beijing: China Building Materials Press.

Mobasher, B. (2019). *Mechanics of Fiber and Textile Reinforced Cement Composites.* New York: CRC Press.

Naaman, A. E. (2010). "Textile reinforced cement composites: competitive status and research directions," in *Proceedings, International RILEM Conference on Material Science,* ed. W. Brameshuber (Aachen: RILEM Publications SARL), 3–22.

Ortlepp, R., and Ortlepp, S. (2017). Textile reinforced concrete for strengthening of RC columns: a contribution to resource conservation through the preservation of structures. *Constr. Build. Mater.* 132, 150–160. doi: 10.1016/j.conbuildmat.2016.11.133

Peled, A., Bentur, A., and Mobasher, B. (2019). *Textile Reinforced Concrete.* New York, NY: CRC Press.

Raoof, S. M., Koutas, L. N., and Bournas, D. A. (2017). Textile-reinforced mortar (TRM) versus fibre-reinforced polymers (FRP) in flexural strengthening of RC beams. *Constr. Build. Mater.* 151, 279–291. doi: 10.1016/j.conbuildmat.2017.05.023

Tran, M. T., Vu, X. H., and Ferrier, E. (2018). Experimental and analytical analysis of the effect of fiber treatment on the thermomechanical behavior of continuous carbon textile subjected to simultaneous elevated temperature and uniaxial tensile loadings. *Constr. Build. Mater.* 183, 32–45. doi: 10.1016/j.conbuildmat.2018.06.114

Triantafillou, T. C. (2016). *Textile Fibre Composites in Civil Engineering.* Duxford: Woodhead Publishing.

Xu, S. L., Shen, L., and Wang, J. (2016). The high-temperature resistance performance of TRC thin-plates with different cementitious materials: experimental study. *Constr. Build. Mater.* 115, 506–519. doi: 10.1016/j.conbuildmat.2016.04.070

Xun, Y., Zhi, Z. D., and Zhang, Q. (2010). Experimental research on flexural behavior of reinforced concrete beams strengthened with textile reinforced concrete sheets. *J. Build. Struct.* 31, 70–76.

Yang, J. M., Wang, L. M., Jin, C., and Sheng, D. (2020). Effect of fly ash on the corrosion resistance of magnesium potassium phosphate cement paste in sulfate solution. *Constr. Build. Mater.* 237:117639. doi: 10.1016/j.conbuildmat.2019.117639

Yin, S. P. (2010). *Research on TRC Mechanical Behavior and Flexural Performance of Concrete Beam Reinforced with TRC.* Doctoral Thesis, Dalian University of Technology, Dalian.

Yin, S. P., Jing, L., Yin, M. T., and Wang, B. (2019). Mechanical properties of textile reinforced concrete under chloride wet-dry and freeze-thaw cycle environments. *Cem. Concr. Comp.* 96, 118–127. doi: 10.1016/j.cemconcomp.2018.11.020

Yin, S. P., Sheng, J., Lv, H. L., and Jia, S. (2015). Flexural behavior of RC beams strengthened with TRC under static loading. *Chn. J. Highway Transport.* 28, 45–53.

Zhang, Q. (2009). *Experimental Study on Flexural Behavior of Reinforced Concrete Beams Strengthened with Textile Reinforced Concrete.* Ph. D. Thesis, Jiangsu University, Zhenjiang.

Zhi, Z. D., Chen, H., Xun, Y., Yang, J. M., and Du, Y. B. (2017). Experimental research on flexural behavior of RC beams strengthened with E-glass textile reinforced fine aggregate concrete sheets used magnesium phosphate cement. *Build. Struct.* 47, 89–93.